

Electronic Supplementary Information

Morphology-Selective Synthesis of $\text{Cu}(\text{NO}_3)_2 \cdot 2.5\text{H}_2\text{O}$ Micro/Nanostructures Achieved by Rational Manipulation of Nucleation Pathways and Their Morphology-Preserved Conversion to CuO Porous Micro/Nanostructures

Feng Feng,^a Muzi Chen,^b and Ji Hong Wu^{a,*}

^aCollege of Chemistry, Chemical Engineering and Materials Science, Soochow University,
199 RenAi Road, Suzhou, Jiangsu, China 215123

^bTesting & Analysis Center, Soochow University, 199 RenAi Road, Suzhou, Jiangsu, China
215123

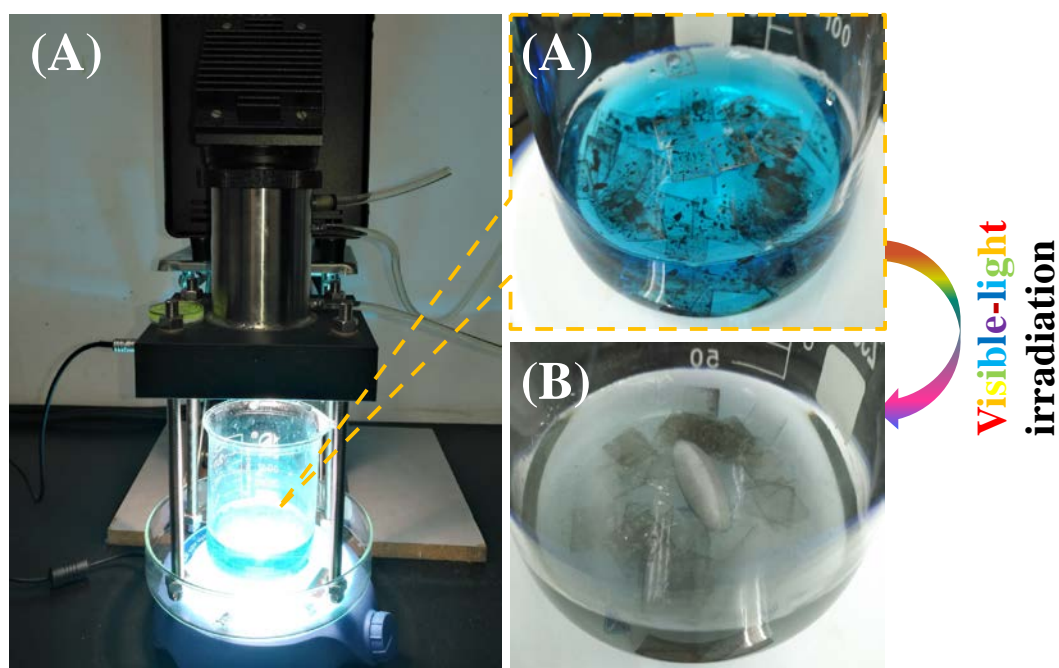


Figure S1 Experimental setup for photocatalytic degradation of MB under visible-light irradiation.

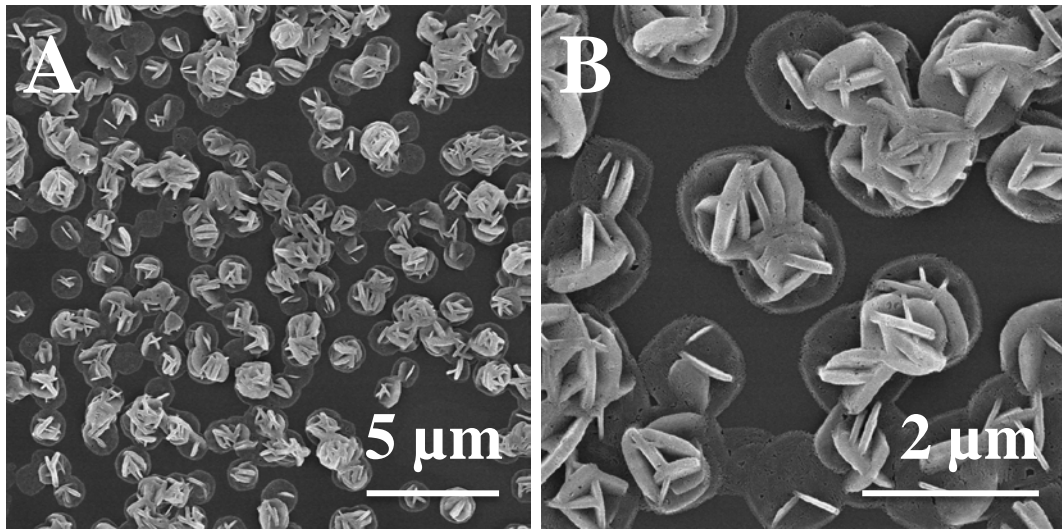


Fig. S2 SEM characterizations of the flower-like hierarchical microspheres prepared from $\text{Cu}(\text{NO}_3)_2$ thin solution layer when a strong N_2 flow was applied. The $\text{Cu}(\text{NO}_3)_2$ thin solution layer was rapidly evaporated in N_2 atmosphere for 5 s. Concentration of $\text{Cu}(\text{NO}_3)_2$: 0.5 M.

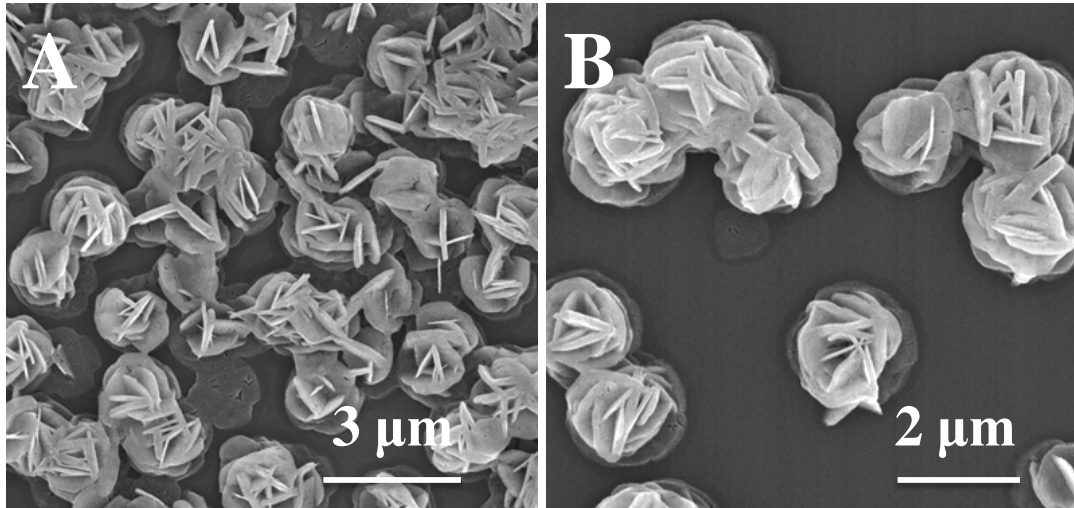


Fig. S3 SEM characterizations of the flower-like hierarchical microspheres prepared from $\text{Cu}(\text{NO}_3)_2$ thin solution layer when a soft N_2 flow was applied. The $\text{Cu}(\text{NO}_3)_2$ thin solution layer was rapidly evaporated in N_2 atmosphere for 30 s. Concentration of $\text{Cu}(\text{NO}_3)_2$: 1.5 M.

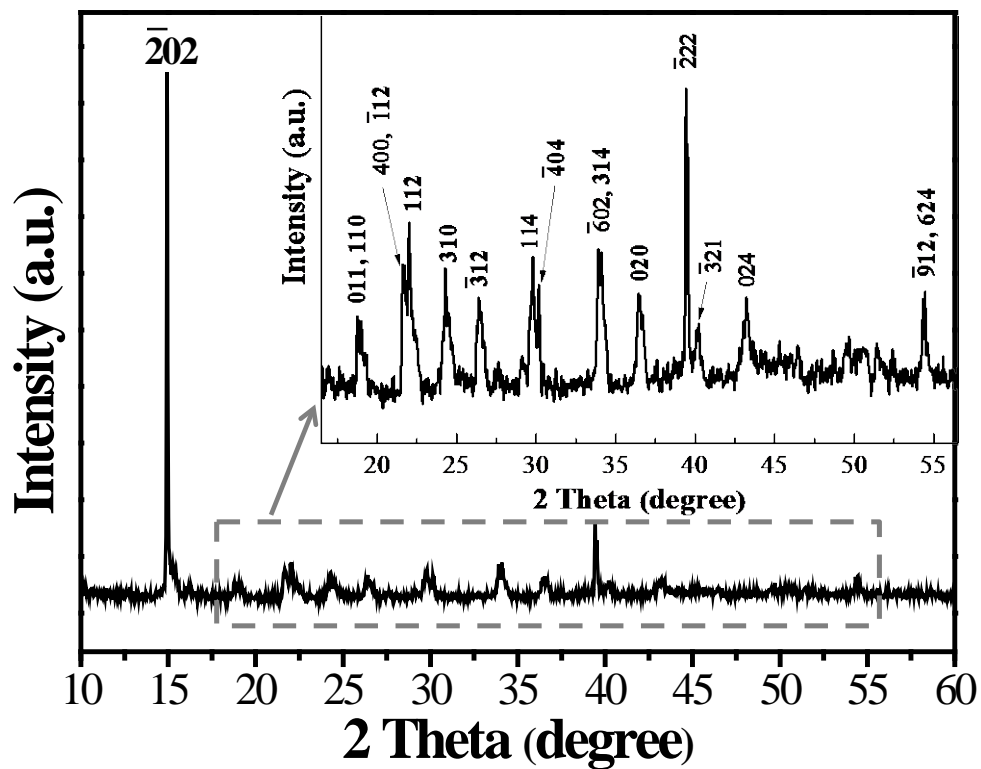


Fig. S4 XRD pattern of the as-prepared $\text{Cu}(\text{NO}_3)_2 \cdot 2.5\text{H}_2\text{O}$ micro/nanostructures with monoclinic crystal symmetry (JCPDS No.: 75-1493; space group: I2/c).

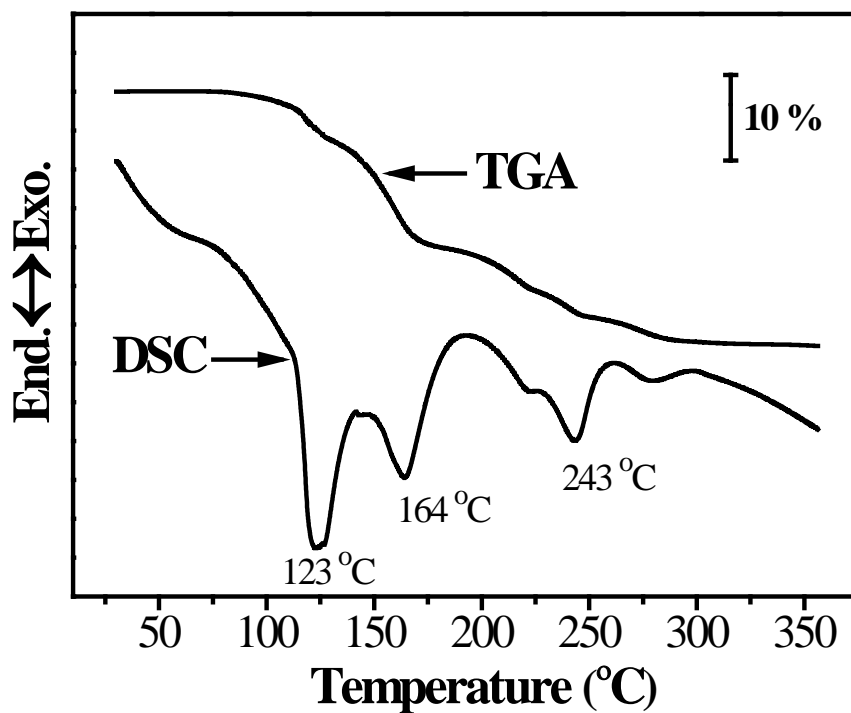


Fig. S5 Simultaneous differential scanning calorimetry-thermogravimetric analysis (DSC-TGA) of the thermal decomposition process of Cu(NO₃)₂·2.5H₂O micro/nanostructures. The DSC-TGA results indicate that the thermal decomposition of Cu(NO₃)₂·2.5H₂O underwent three stages, Eventually, Cu(NO₃)₂·2.5H₂O was decomposed to CuO in the temperature window of 195-290 °C centred at 243 °C.

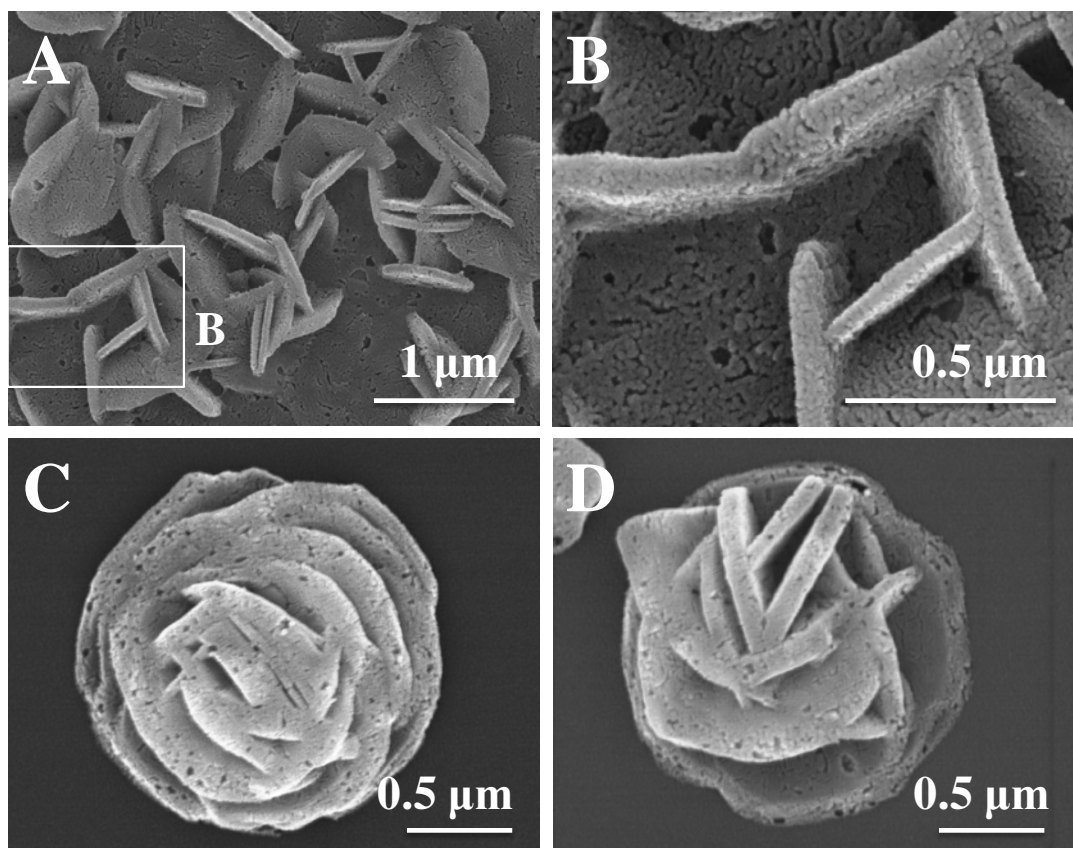


Fig. S6 SEM characterizations of CuO porous nanoplates (A,B) and CuO porous microspheres (C,D).

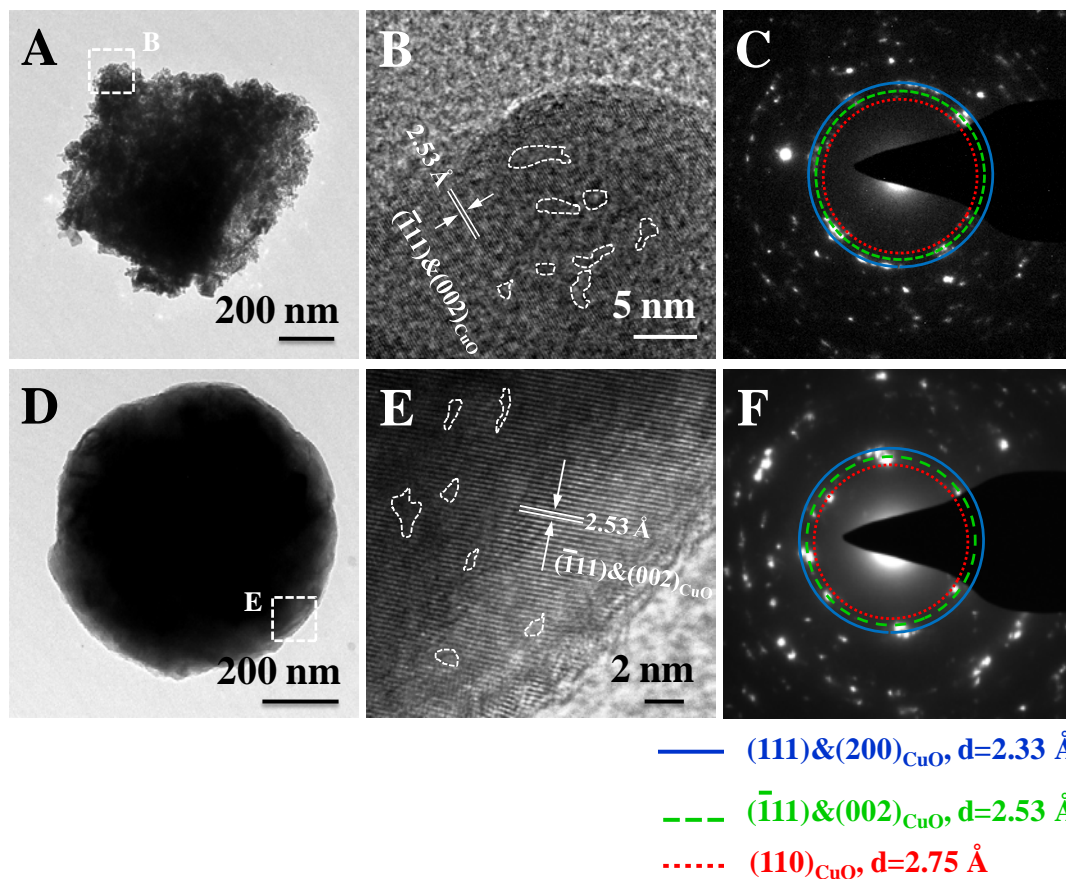
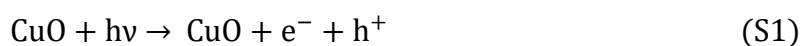
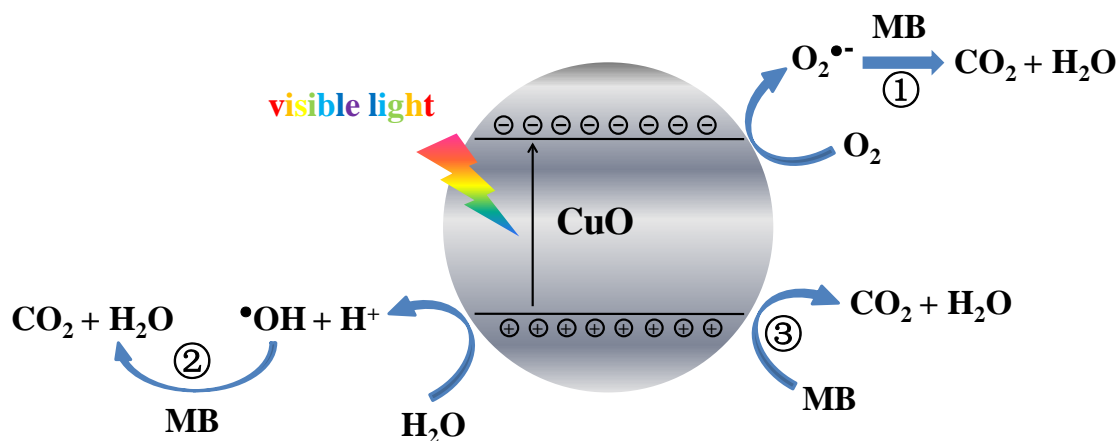


Fig. S7 (A-C) TEM characterizations of CuO porous nanoplates: (A) TEM image. (B) HRTEM image. The irregular-shaped circles in white dash lines highlight where the nanopores locate. (C) Selected-area electron diffraction (SAED) pattern. (D-F) TEM characterizations of CuO porous microspheres: (D) TEM image. (E) HRTEM image. The irregular-shaped circles in white dash lines highlight where the nanopores locate. (F) SAED pattern.

Photocatalytic mechanisms

The photocatalytic degradation of MB is based on a photochemical mechanism involving photoinduced charge generation, separation, and migration. As a narrow band gap semiconductor, CuO can be excited under visible-light irradiation. Excitons (i.e., electron–hole pairs) are generated upon the absorption of photons (eq. S1). The electrons and holes separate from each other and migrate to CuO surfaces. On CuO surfaces, the electrons are captured by oxygen molecules—the surface-absorbed O₂ molecules and/or the O₂ molecules dissolved in solution. The reaction of electrons and O₂ will create the superoxide radical anions (O₂^{•-}) (eq. S2). The photoinduced holes will react with H₂O molecules to form the energetic oxidative hydroxyl radicals (•OH) (eq. S3). Eventually, the MB molecules will be quickly mineralized into CO₂ and H₂O under the conjoint attack from the energetic oxidative species, including O₂^{•-}, •OH, and holes (h⁺) (eqs. S4-6).¹⁻⁵ Based on the above discussion, schematic mechanistic illustrations were proposed for visible-light degradation of MB in the presence of CuO photocatalyst (Scheme S1).





Scheme S1 Proposed schematic mechanistic illustrations for visible-light degradation of MB in the presence of CuO photocatalyst.

References

1. S. Gao, Z. Li, K. Jiang, H. Zeng, L. Li, X. Fang, X. Jia and Y. Chen, *J. Mater. Chem.*, 2011, **21**, 7281-7288.
2. W.-N. Wang, C.-X. Huang, C.-Y. Zhang, M.-L. Zhao, J. Zhang, H.-J. Chen, Z.-B. Zha, T. Zhao and H.-S. Qian, *Applied Catalysis B: Environmental*, 2018, **224**, 854-862.
3. F. Zhang, W. N. Wang, H. P. Cong, L. B. Luo, Z. B. Zha and H. S. Qian, *Particle & Particle Systems Characterization*, 2017, **34**.
4. F. Zhang, C.-L. Zhang, H.-Y. Peng, H.-P. Cong and H.-S. Qian, *Particle & Particle Systems Characterization*, 2016, **33**, 248-253.
5. S. N. Guo, Y. L. Min, J. C. Fan and Q. J. Xu, *ACS applied materials & interfaces*, 2016, **8**, 2928-2934.